Iron Release from the Siderophore Pyoverdine in Involves Three New Actors: FpvC, FpvG, and FpvH

Géraldine Ganne, Karl Brillet, Beata Szafarowicz Basta, Béatrice Roche, Françoise Hoegy, Véronique Gasser, Isabelle Schalk

Iron release from the siderophore pyoverdine in *Pseudomonas aeruginosa* involves three new actors FpvC, FpvG and FpvH

Géraldine Ganne[1, 2, #], Karl Brillet[1, 2, #], Beata Basta[1, 2], Béatrice Roche[1, 2], Françoise Hoegy[1, 2], Véronique Gasser[1, 2], Isabelle J. Schalk[1, 2, *]

[1] Université de Strasbourg, UMR7242, ESBS, Bld Sébastien Brant, F-67413 Illkirch, Strasbourg, France

[2] CNRS, UMR7242, ESBS, Bld Sébastien Brant, F-67413 Illkirch, Strasbourg, France

[#] Contributed equally to the manuscript

[*] To whom correspondence should be addressed: Isabelle J. Schalk, UMR 7242, ESBS, Blvd Sébastien Brant, BP 10412, F-67413 Illkirch, Strasbourg, France. Tel: 33 3 68 85 47 19; Fax: 33 3 68 85 48 29; E-mail: isabelle.schalk@unistra.fr.

ABSTRACT

Siderophores are iron chelators produced by bacteria to access iron, an essential nutriment. Pyoverdine (PVDI), the major siderophore produced by *Pseudomonas aeruginosa* PAO1, consists of a fluorescent chromophore linked to an octapeptide. The ferric-form of PVDI is transported from the extracellular environment into the periplasm by the outer membrane transporter, FpvA. Iron is then released from the siderophore in the periplasm by a mechanism that does not involve chemical modification of the chelator, but an iron reduction step. Here, we followed the kinetics of iron release from PVDI, *in vitro* and in living cells, by monitoring its fluorescence (as apo PVDI is fluorescent whereas PVDI-Fe(III) is not). Deletion of the inner membrane proteins *fpvG* (PA2403) and *fpvH* (PA2404) affected ^{55}Fe uptake *via* PVDI and completely abolished PVDI-Fe dissociation, indicating that these two proteins are involved in iron acquisition *via* this siderophore. PVDI-Fe dissociation studies, using an *in vitro* assay, showed that iron release from this siderophore requires the presence of an iron reducer (DTT) and an iron chelator (ferrozine). In this assay, DTT could be replaced by the inner membrane protein, FpvG, and ferrozine by the periplasmic protein, FpvC, suggesting that FpvG acts as a reductase and FpvC as an Fe^{2+} chelator in the process of PVDI-Fe dissociation in the periplasm of *P. aeruginosa* cells. This mechanism of iron release from PVDI is atypical among Gram-negative bacteria, but seems to be conserved among Pseudomonads.

INTRODUCTION

Pseudomonas aeruginosa, an opportunistic Gram-negative human pathogen, requires iron for its growth, as do all living organisms, because this nutrient is a co-factor for many enzymes involved in fundamental biological processes. Its intracellular concentration in *P. aeruginosa* cells has been estimated to be between 10^{-3} and 10^{-4} M.[1] However, iron availability in the various bacterial environments is severely limited: iron(II) is rapidly oxidized to iron(III) in the presence of oxygen, and precipitates as a polymeric oxyhydroxide. Consequently, bacteria have developed several efficient strategies for facilitating access to this essential element. One of the most commonly used strategies involves the synthesis of siderophores and their release into the bacterial environment.[2] These molecules, produced by most bacteria, have various chemical structures, but have in common a low molecular weight (200 to 2000 Da) and an extremely high affinity for ferric iron, with, for example, K_a values of 10^{43} and 10^{32} M^{-1} for enterobactin and pyoverdine, respectively.[3,4] All fluorescent *Pseudomonas* species produce and secrete specific pyoverdines as their principal siderophores. These siderophores have similar structures: a specific peptide of six to twelve amino acids (characteristic of each pseudomonad species) linked to a chromophore derived from 2,3-diamino-6,7-dihydroxyquinoline, rendering the molecule both colored and fluorescent.[5] Pyoverdine I (PVDI), the siderophore produced by *P. aeruginosa* PAO1, is a partially cyclic octapeptide linked to the chromophore.[6] The pyoverdine pathway of *P. aeruginosa* PAO1 is the only such pathway to have been investigated at the molecular level for the biosynthesis of the siderophore and the mechanism of iron acquisition.

Siderophores chelate iron in the extracellular medium and the resulting ferric-siderophore complex is then transported back into the bacteria. This uptake always involves a specific outer membrane transporter,[7] FpvAI[8,9] and FpvB[10] in the case of PVDI-Fe by *P. aeruginosa*. The protonmotive force of the inner membrane drives this transport across the

outer membrane *via* an inner membrane complex comprised of TonB, ExbB, and ExbD.[11] Once in the periplasm, the fate of the ferric-siderophore complexes is very strain- and siderophore-specific (for a review see[12]). For example, iron dissociates from the siderophore in the periplasm for the pyoverdine[13,14] and citrate[15] iron uptake pathways in *P. aeruginosa*. For the ferrichrome[16,17] and enterobactin[4] pathways of *Escherichia coli*, the ferri-siderophore complexes must cross the inner membrane and iron is released from the chelator only in the bacterial cytoplasm. Bacterial ferric-siderophore dissociation mechanisms in the bacterial periplasm or cytoplasm have received little attention, and this step has been investigated for only a few siderophore pathways: the enterobactin, salmochelin, and ferrichrome pathways and their analogues.[12] These studies indicate that iron is released either by hydrolysis or by modification of the siderophore scaffold, and/or by reduction of the coordinated ferric iron into ferrous iron.

For PVDI, we have previously shown that iron is released from the siderophore in the periplasm *via* a mechanism that does not involve chemical siderophore modification, but an apparent reduction of iron.[13,14] The apo siderophore is then recycled into the extracellular medium by PvdRT-OpmQ, an ATP-dependent efflux pump.[14,18,19] The cellular location of PVDI-Fe dissociation was determined using gallium (Ga^{3+}), a metal that cannot be removed from PVDI by reduction (Ga is found primarily in the +3 oxidation state and cannot be reduced into Ga^{2+}). PVDI-Ga was taken up by *P. aeruginosa*, but no dissociation occurred, and PVDI-Ga accumulated in the periplasm, suggesting that metal release from PVDI occurs in this cell compartment.[13,14] The proteins and the precise mechanism involved in iron reduction and release from PVDI have not yet been identified.

Here, we investigated the involvement of the PA2403-10 genes (*fpvGHJKCDEF,* Figure 1A) in iron release from PVDI in *P. aeruginosa* periplasm. The mutation of PA2403 and PA2404 (coding for FpvG and FpvH, respectively) completely abolished PVDI-Fe

dissociation, substantially decreasing the cytoplasmic assimilation of ^{55}Fe *via* PVDI in *P. aeruginosa* cells. Moreover, *in vitro*, the inner membrane protein FpvG acted as an iron reductase and the periplasmic binding protein FpvC as an iron chelator in the mechanism of iron release from PVDI. Altogether, these combined *in vivo* and *in vitro* data highlight the key roles for the periplasmic protein FpvC and the inner membrane proteins FpvG and FpvH in the process of iron release from PVDI in *P. aeruginosa* cells.

RESULTS & DISCUSSION

fpvGHJK genes characteristics. All genes involved in the PVDI pathway are found in the same locus of the *P. aeruginosa* genome and their biological functions have been identified for many of them but the PA2403-06 genes. The PA2403-06 sequence is separated by 31pb from the PA2407-10 operon (Figure 1A and http://www.pseudomonas.com) coding for an ABC transporter composed of a permease, FpvE (PA2409), and an ATPase, FpvD (PA2408), with two periplasmic binding proteins, FpvC (PA2407) and FpvF (PA2410), involved in iron transport from the periplasm into the cytoplasm after its release from PVDI.[20] The adjacent PA2403-06 operon of unknown function codes for four proteins: FpvG (PA2403; 45 kDa), FpvH (PA2404; 19.9 kDa), FpvJ (PA2405; 11.4 kDa), and FpvK (PA2406; 19.4 kDa). The *fpvGHJK* genes may play a role in the mechanism of iron release from PVDI as they are localized next to the *fpvCDEF* genes. The start and stop codons of the four *fpvGHJK* genes overlap, suggesting that their expression may be coupled.

Secondary structure prediction performed by several algorithms (Phyre2, XtalPred-RF, TMHMM, TMpred, and CCTOP) indicate that FpvG is an inner membrane protein composed of four transmembrane α helices (TM1: amino acids 12-36; TM2: amino acids 146-167; TM3: amino acids 187-217; and TM4: amino acids 336-363) and two putative periplasmic domains (the first from residues 37 to 145 and the second from residues 218 to 335) (Figure 1B). The two putative periplasmic domains of FpvG have the same secondary organization and are composed of an α helix and four putative β strands. Results from a FFASO3 search in PfamA27U revealed that FpvG significantly matches a transmembrane ascorbate ferric-reductase (from *Arabidopsis thaliana*) (score -9.640), belonging to the eukaryotic Cytochrome b561 family (transmembrane electron transport protein involved in iron reductase activities) (Su and al., 2006). However none of the bioinformatics analysis that we carried out allowed indicated that FpvG possesses a heme binding site. The secondary

structure predictions for FpvH and FpvK suggest a similar organization with a putative transmembrane α helix (amino acids 21-41 for FpvH and amino acids 15-35 for FpvK) and a potential periplasmic domain (amino acids 42-179 for FpvH and amino acids 36-186 for FpvK). A signal sequence (amino acids 1-25) was predicted by SignalP for FpvJ, suggesting periplasmic localization for this protein.

***fpvGHJK deletion affects ^{55}Fe uptake in* P. aeruginosa.** We assessed the ability of mutants carrying single *fpvG*, *fpvH*, *fpvJ*, and *fpvK* deletions or a simultaneous deletion of all four *fpvGHJK* genes to transport and accumulate iron in the presence of PVDI, in a PVDI-^{55}Fe uptake assay. The PVDI concentration was precisely controlled by performing the experiment using the PVDI-negative *P. aeruginosa* mutant Δ*pvdF* and its *fpvG*, *fpvH*, *fpvJ*, and *fpvK* deletion derivatives (Δ*pvdF*Δ*fpvG,* Δ*pvdF*Δ*fpvH,* Δ*pvdF*Δ*fpvJ,* Δ*pvdF*Δ*fpvK* and Δ*pvdF*Δ*fpvGHJK)*. As a negative control, we also used the Δ*pvdF*Δ*fpvA* strain carrying the deletion of the outer membrane transporter FpvA as a negative control. We incubated bacteria in the presence of 200 nM PVDI-^{55}Fe and monitored the radioactivity incorporated into the cells. After 30 min, 95 pmol ^{55}Fe was incorporated into Δ*pvdF* cells, whereas we observed no ^{55}Fe accumulation in the *fpvA* deletion mutant Δ*pvdF*Δ*fpvA* (Figure 2A) or in the Δ*pvdF* cells when they were incubated in the presence of CCCP, a proton motive force inhibitor that blocks all TonB-dependent transport.[21] Deletion of *fpvG* reduced ^{55}Fe uptake by 44 and 46% in the Δ*pvdF*Δ*fpvG* and Δ*pvdF*Δ*fpvGHJK* strains, respectively (Figure 2A). We only observed this phenotype in a highly iron-restricted medium, such as CAA, but not in a medium such as succinate (less iron-restricted, Supplementary Figure 2). Deletion of *fpvH* and *fpvJ* reduced ^{55}Fe uptake by 19 and 17%, respectively. Finally, deletion of *fpvK* had no effect on ^{55}Fe uptake *via* the PVDI pathway. In conclusion, among the deletion of the four genes *fpvG, fpvH, fpvJ, and fpvK*, we observed the strongest inhibition of iron uptake (equivalent to that

observed for the *fpvGHJK* deletion) for the deletion of *fpvG*, suggesting a key role for this protein in the PVDI pathway; *fpvH* and *fpvJ* also play a role, but of lower importance.

We repeated the uptake experiments in the presence of 200 nM PVDI-^{55}Fe and fractionated the cells after 30 min incubation with the siderophore-iron complex, and measured the radioactivity in each cell compartment (periplasm, cytoplasm and membranes) (Figure 2B). For the PVDI-deficient strain Δ*pvdF*, most of ^{55}Fe was found in the cytoplasm or associated with the membrane (41 and 32%, respectively) and only 10% in the periplasm. For the corresponding FpvA mutant ((Δ*pvdF*Δ*fpvA*), all the radioactivity remained outside the bacteria. For the strains deleted for *fpvG* (Δ*pvdF*Δ*fpvG* and Δ*pvdF*Δ*fpvGHJK*), there was two-fold lower ^{55}Fe accumulation in the cytoplasm and five-fold lower association with the membranes than for Δ*pvdF*. In parallel, there was a four to five-fold increase of ^{55}Fe accumulation in the periplasm, suggesting that the metal is blocked in this cell compartment in the absence of FpvG.

Overall, these data indicate that FpvG, and to a lower extend FpvH and FpvJ, are involved in iron acquisition by the siderophore PVDI and play a role in a step necessary for or preceding iron translocation from the periplasm into the cytoplasm of *P. aeruginosa* by the ABC transporter, FpvDE, and its two periplasmic proteins, FpvC and FpvF.[20]

Involvement of fpvGHJK and fpvCDEF in PVDI-Fe dissociation. PVDI is a fluorescent siderophore with experimentally exploitable spectral characteristics, due to the presence of the chromophore derived from 2,3-diamino-6,7-dihydroxyquinoline. Indeed, the apo form of PVDI is fluorescent (excitation at 400 nm, emission at 447 nm), but the PVDI-Fe complex is not.[13,22,23] The release of iron from the PVDI-Fe complex can therefore be followed in real time by monitoring the fluorescence of apo PVDI in living bacteria.[13] We further investigated the role of the FpvG, FpvH, FpvJ, and FpvK proteins in iron uptake by PVDI in *P.*

aeruginosa cells, by incubating our different mutants in the presence of 120 nM PVDI-Fe and monitoring the fluorescence of PVDI (Figure 3A). The only source of siderophore present was the PVDI-Fe complex added to the cells at the beginning of the experiment. Consistent with previous findings,[13] fluorescence increased following the addition of PVDI-Fe to Δ*pvdF* cells (Figure 3A, green curve). This corresponds to the dissociation of PVDI-Fe (formation of fluorescent apo PVDI) in the bacterial periplasm.[13] There was no increase of fluorescence in the absence of FpvA (Δ*pvdF*Δ*fpvA* strain, Figure 3A, gray curve), because no PVDI-Fe could be transported into the bacteria. Deletion of the *fpvGHJK* genes almost completely inhibited (92%) PVDI-Fe dissociation relative to the Δ*pvdF* mutant (Figure 3A, blue curve). The use of single deletion mutants of the *fpvGHJK* cluster showed that the FpvG and FpvH proteins are important for the process of iron release from PVDI in *P. aeruginosa* cells: deletion of these two genes completely abolished PVDI-Fe dissociation as for the *fpvA* or *fpvGHJK* mutants (Figure 3A, red and orange curves). Complementation of these two mutations with a plasmid carrying the *fpvG or fpvH* genes, completely restored PVDI-Fe dissociation for *fpvG* and partially for *fpvH* (Supplementary Figure 3). For the Δ*pvdF*Δ*fpvJ* and Δ*pvdF*Δ*fpvK* strains, we observed 57 and 74% inhibition of PVDI-Fe dissociation, indicating that the FpvJ and FpvK proteins also play a role in the dissociation of iron from PVDI, but to a lesser extent than FpvG and FpvH (Figure 3A, pink and purple curves). All four mutants of the *fpvCDEF* operon tested (Δ*pvdF*Δ*fpvC*, Δ*pvdF*Δ*fpvDE*, Δ*pvdF*Δ*fpvF*, and Δ*pvdF*Δ*fpvCDEF*) showed 40% inhibition of PVDI-Fe dissociation (Figure 3B).

Iron dissociation from PVD is followed by recycling of the apo siderophore into the extracellular medium *via* the efflux system PvdRT-OpmQ. Recycling can be followed in real time, *in vivo*, by monitoring the apparition of fluorescence, corresponding to apo PVDI in the extracellular medium of *P. aeruginosa* cells. As above, we incubated the different mutants in the presence of 120 nM PVDI-Fe (Figure 3C), collected aliquots at various intervals, pelleted

the bacteria, and measured the fluorescence at 447 nm in the supernatant. Extracellular fluorescence increased for the Δ*pvdF* cells (Figure 3C, green curve), but not for the control samples without cells (Figure 3C, black curve) or PVDI-Fe (data not shown). This increase in fluorescence is due to recycling of metal-free PVDI from the periplasm into the extracellular medium after the release of iron from PVDI in the bacteria.[18] For Δ*pvdF*Δ*fpvG* or Δ*pvdF*Δ*fpvH*, PVDI recycling was completely abolished (Figure 3C, red and orange curves), consistent with the results of the dissociation experiment. The rate of the increase of extracellular fluorescence was considerably lower for Δ*pvdF*Δ*fpvJ* and Δ*pvdF*Δ*fpvK* (50 and 66%, respectively) compared to the experiment with Δ*pvdF* (Figure 3C, pink and purple curves), indicating that siderophore recycling was affected to the same extent as PVDI-Fe dissociation for these mutations. Concerning the ABC transporter FpvDE and its two periplasmic proteins, the Δ*pvdF*Δ*fpvC*, Δ*pvdF*Δ*fpvDE*, Δ*pvdF*Δ*fpvF*, and Δ*pvdF*Δ*fpvCDEF* mutants showed phenotypes for apo PVDI recycling that were equivalent to the kinetics of PVDI-Fe dissociation with 45% inhibition (Figure 3D).

In conclusion, these data show that FpvG and FpvH play a key role in the mechanism of iron release from the siderophore in the bacterial periplasm. In the absence of FpvG and FpvH, PVDI can no longer release iron, and consequently, apo PVDI can no longer be recycled into the extracellular medium. The inner membrane protein FpvK and the periplasmic proteins FpvJ, FpvC, and FpvF also play a role, but their deletion has a smaller effect on the rate of PVDI-Fe dissociation. Surprisingly, even the ABC transporter FpvDE, described to be involved in the transport of siderophore-free iron across the inner membrane into the cytoplasm,[20] is also important for the mechanism of iron release from the siderophore. The absence of this transporter may block steps upstream of iron translocation across the cytoplasmic membrane, preventing the further transport of siderophore-free iron.

In vitro*, DTT and ferrozine promotes iron dissociation from PVDI.* Iron release from siderophores in bacterial cells often involves an iron reduction step and an Fe^{2+} chelator, as ferric-siderophore complexes are extremely stable.[12] Previous findings from our group, based on PVDI-Ga complex uptake by *P. aeruginosa* cells, showed that iron reduction is required for the dissociation of PVDI-Fe and that it occurs in the bacterial periplasm.[13,14]

We further investigated the molecular mechanism involved in iron release from PVDI in *P. aeruginosa* cells by studying PVDI-Fe dissociation *in vitro,* using the fluorescent properties of PVDI[13] in the presence of DTT as the reducing agent and ferrozine as the ferrous iron chelator. Ferrozine is used as a Fe^{2+} chelating reagent and indicator because it forms a stable magenta-colored complex (absorption peak at 562 nm) with ferrous iron.[24] Incubation of PVDI-Fe in the presence of DTT led to an increase in fluorescence, corresponding to the formation of metal-free PVDI (Figure 4A, blue curve and solid line). The addition of ferrozine led to a larger increase in fluorescence (Figure 4A, purple curve with solid line), suggesting that ferrozine increases the efficiency of PVDI-Fe dissociation in the presence of DTT, probably by chelating the ferrous iron that is formed. We followed the formation of the ferrozine-Fe^{2+} complex by monitoring the absorbance at 562 nm over time (Figure 4A, purple curve with dotted line). The kinetics of the formation of the ferrozine-Fe^{2+} complex were similar to those for the formation of metal-free PVDI (Figure 4A). We next assessed iron release from PVDI in the presence of ascorbic acid, a compound that simultaneously acts as a reducing agent and ferrous iron chelator. Iron was released from PVDI more efficiently by ascorbic acid than DTT (Figure 4B, green curve). The addition of ferrozine increased the amount of apo PVDI formed (Figure 4B, red curve), similar to DTT.

Thus, Fe^{3+} can be removed from PVDI by metal reduction, and the rate of dissociation is higher in the presence of an Fe^{2+} chelator. Previous studies have shown that PVDI also chelates Fe^{2+}, in addition to Fe^{3+},[25] suggesting that only small amounts of metal-free PVDI are

formed in the absence of Fe^{2+} trapping by ferrozine or another Fe^{2+} chelator. In the presence of ferrozine or ascorbic acid, ferrozine-Fe^{2+} and ascorbic-Fe^{2+} complexes are formed and iron is consequently released more efficiently from PVDI. This suggests that efficient PVDI-Fe dissociation *in vivo* requires both Fe^{3+} reduction and an exchange process in which the Fe^{2+} formed interacts with another chelator with a higher affinity for the reduced metal than PVDI.

FpvC facilitates DTT-dependent PVDI-Fe dissociation, like ferrozine. Sequence alignments clearly showed that FpvC has homology with metal-binding periplasmic proteins[20] and may act as the ferrous iron chelator in the mechanism of iron release from PVDI. Similar to ferrozine, the addition of purified FpvC enhanced PVDI-Fe dissociation in the presence of excess DTT (Figure 4C, green curve), certainly by chelating the ferrous iron formed. FpvC appears to be as efficient in this process as ferrozine, since 10 μM of FpvC and 10 μM ferrozine displayed equivalent kinetics for PVDI-Fe dissociation (Figure 4C). There was no increase in fluorescence at 447 nm when PVDI-Fe was incubated in the presence of FpvC, in the absence of DTT (Figure 4C, orange curve), clearly indicating that FpvC alone is unable to remove iron from PVDI. Finally, we mutated six His residues of FpvC, potentially involved in iron chelation based on sequence alignments with metal binding periplasmic proteins, into Gly (Figure 1C). This mutated FpvC protein ($FpvC_{mut}$) lost the ability to activate DTT-dependent PVDI-Fe dissociation (Figure 4D, green curve with dots), confirming that FpvC acts as an iron chelator in the mechanism of iron release from PVDI.

FpvG promotes PVDI-Fe dissociation, likely playing the role of a reductase. In attempts to overexpress FpvG and FpvH in *E. coli*, we succeeded only for FpvG. Western blot analyses of membrane preparations of BL21(DE3) carrying the plasmid pET29a(+)*fpvG*His_6 confirmed that FpvG is a membrane protein (Figure 5). We observed no expression of FpvH. We further

investigate the role of FpvG in the PVDI pathway, by following PVDI-Fe dissociation by fluorescence in the presence of cytoplasmic membranes isolated from *E. coli* strains expressing, or not, FpvG. We observed increased fluorescence, corresponding to the release of iron from PVDI, only with the membranes isolated from *E. coli* cells expressing FpvG (Figure 4E, red curve). There was no increase of fluorescence with membranes from *E. coli* cells not carrying the pET29a(+)FpvGHis$_6$ plasmid (Figure 4E, orange curve), indicating that FpvG is responsible for the observed PVDI-Fe dissociation and no other *E. coli* membrane proteins. The kinetics of PVDI-Fe dissociation in the presence of FpvG were faster, with a higher plateau, than in the presence of DTT (Figure 4E, blue curve) indicating that FpvG acts like DTT as a reducer in this *in vitro* PVDI-Fe dissociation assay. We also extracted FpvG from the membranes by 1% DDM and purified it using a HisTrap HP column, but observed no PVDI-Fe dissociation with the purified FpvG (data not shown). The reductase activity of FpvG is likely unstable in the presence of oxygen and detergent or requires stabilization by FpvH, FpvJ, and FpvK. The ability to replace the role of DTT in *in vitro* PVDI-Fe dissociation assays and the absence of PVDI-Fe dissociation in a *fpvG* mutant strongly suggest that FpvG is the reductase in the process of PVDI-Fe dissociation in *P. aeruginosa* cells. In agreement with its probable role as a reductase, results from a FFASO3 search in PfamA27U revealed that FpvG significantly matches a transmembrane ascorbate ferric-reductase (from *Arabidopsis thaliana*) (score -9.640), belonging to the eukaryotic Cytochrome b561 family. Cytochrome b561 family members are transmembrane electron transport proteins involved in iron reductase activities and are characterized by a central transmembrane four-helix core containing four highly conserved histidine residues anchoring two heme groups (Su and al., 2006). However none of the bioinformatics analysis that we carried out indicated that FpvG possesses a heme binding site.

FpvG-promoted PVDI-Fe dissociation is not enhanced by the addition of the Fe^{2+}

chelator ferrozine (Figure 4E, purple curve), suggesting that ferrous iron is not liberated into the media in the presence of FpvG. Ferrous iron may remain bound to FpvG, chelated either by the protein or in a FpvG-PVDI complex with a mixed coordination shell for iron, involving residues of FpvG and the L-formyl-N^{δ}-hydroxyornithines of PVDI (the catechol group of PVDI is no longer involved in chelation, as the siderophore became fluorescent in the presence of FpvG).

This ability of FpvG to act as a reductase in *in vitro* PVDI-Fe dissociation assays raises many questions. Further biophysical studies will be necessary to investigate the interaction between PVDI-Fe and FpvG, the location of the siderophore binding site on FpvG, and the precise enzymatic mechanism that allows the release of iron from PVDI. Previous studies have clearly shown that PVDI-Fe dissociation *in vivo* involves no chemical modification or degradation of PVDI, only an iron reduction step.[13] Altogether, the *in vivo* and *in vitro* data show FpvG to be the reductase in the mechanism of PVDI-Fe dissociation in *P. aeruginosa* cells. The *fpvG* gene is conserved in most *Pseudomonas* species, with the exception of the non-fluorescent *Pseudomonas stutzeri* and *Pseudomonas mendocina*, suggesting that the present mechanism may be conserved among Pseudomonads.

Why is the periplasmic protein FpvC unable to promote FpvG-dependent PVDI-Fe dissociation? The data presented in Figure 4C and 4D show that FpvC can act like ferrozine in DTT-promoted PVDI-Fe dissociation *in vitro*. Surprisingly, FpvC slowed down PVDI-Fe dissociation when DTT was replaced in the assay by FpvG (Figure 4F, green curve). Addition of the purified periplasmic siderophore binding protein FpvF,[20] also slowed down the kinetics of PVDI-Fe dissociation (Figure 4F, blue curve), likely because of competition with FpvG for binding to PVDI-Fe. Finally, the addition of both FpvC and FpvF substantially reduced PVDI-Fe dissociation in the presence of FpvG (Figure 4F, orange curve). Previous *in vitro*

and *in vivo* studies have shown that FpvC and FpvF can simultaneously interact with and bind to PVDI-Fe in a FpvC-FpvF-PVDI-Fe complex.[20] FpvC and FpvF likely form a FpvC-FpvF complex, which probably has a higher affinity for PVDI-Fe than FpvG, inhibiting FpvG-dependent iron dissociation. Under such experimental conditions, PVDI-Fe would be scavenged by FpvC-FpvF and would be unable to interact with FpvG. Moreover, the data presented in Figures 2 and 3, show that FpvH, and to a lesser extent, FpvJ and FpvK, are also involved in iron acquisition by PVDI and may be involved in PVDI-Fe dissociation. One of these three proteins may aid the transfer of ferrous iron from FpvG to FpvC. In further studies, it will be important to investigate the precise role of each protein of the *fpvGHJK* operon, whether they form an inner membrane complex, and how they interact with each other, as well as with the periplasmic binding proteins FpvC and FpvF.

CONCLUSION

This study improves our understanding of the mechanism implicated in the release of iron from PVDI in *P. aeruginosa* cells. The PVDI-Fe complex is probably first scavenged by the periplasmic FpvC-FpvF complex, as previously proposed,[20] following translocation across the outer membrane from the extracellular medium into the bacterial periplasm *via* the TonB-dependent transporter FpvA. Iron release from PVDI occurs in the bacterial periplasm and involves an iron reduction step[13] and the expression of FpvG, FpvH, FpvJ, and FpvK (Figure 3). FpvG acts as an iron reductase and FpvH, FpvJ and FpvK proteins probably act as partners of FpvG, since FpvG alone is able to replace DTT in *in vitro* PVDI-Fe dissociation assays (Figure 4E). Iron can then be transferred to another chelator, FpvC, as PVDI has a lower affinity for ferrous than ferric iron. It is possible that FpvC then brings the iron ion to the ABC transporter FpvDE for its translocation into the cytoplasm.[20] Apo PVDI is recycled into the extracellular medium by the efflux pump PvdRT-OpmQ to start a new iron uptake

cycle.[14,18,19] FpvG appears to be a reductase but requires the other proteins, FpvH, FpvJ, and FpvK, as partners. Further studies will be necessary to understand the exact enzymatic reaction carried out by FpvG, the exact roles of FpvH, FpvJ, and FpvK, and how these proteins interact and transfer iron from PVDI to FpvC. Such a periplasmic mechanism for ferric-siderophore dissociation involving the inner membrane reductase FpvG has never been described for any other iron uptake pathway in Gram-negative bacteria and is probably a specific system conserved among pyoverdine producing Pseudomonads.

METHODS

Chemicals, growth media, and siderophores. The protonophore CCCP was purchased from Sigma. $^{55}FeCl_3$ was obtained from Perkin Elmer Life and Analytical Sciences, in solution, at a concentration of 71.1 mM, with a specific activity of 10.18 Ci g^{-1}. PVDI was purified as previously described.[26] LB broth and LB broth agar medium were purchased from Difco and were used as nutriment-rich medium in all experiments.

Escherichia coli strains were routinely grown in LB broth at 37°C. For cultures of *P. aeruginosa* strains in iron-limited media, bacteria were first grown in LB broth overnight at 30°C. The bacteria were then washed in succinate medium (6.0 g L^{-1} K_2HPO_4, 3.0 g L^{-1} KH_2PO_4, 1.0 g L^{-1} $[NH_4]_2SO_4$, 0.2 g L^{-1} $MgSO_4.7H_2O$, 4.0 g L^{-1} sodium succinate; the pH was adjusted to 7.0 by the addition of NaOH) or CAA medium (casamino acid medium, composition: 5 g L^{-1} low-iron CAA (Difco), 1.46 g L^{-1} K_2HPO_4 $3H_2O$, 0.25 g L^{-1} $MgSO_4$ $7H_2O$) and incubated for 24 h at 30°C. Afterwards, bacteria were diluted to 0.1 $OD_{600\ nm}$ in fresh succinate or CAA medium and incubated at 30°C overnight. Media were supplemented as necessary with 150 μg mL^{-1} carbenicillin. CAA is a more highly iron restricted medium

than succinate medium with iron concentrations of 20 nM and 300 nM, respectively.[1] The iron concentration in LB is approximately 4 μM.[1]

Gene deletion mutant construction. All DNA amplifications for cloning were performed using Phusion High-Fidelity DNA polymerase (ThermoFisher Scientific) and genomic DNA of the PAO1 strain. Restriction endonucleases were purchased from ThermoFisher Scientific and T4 DNA ligase from Takara. All enzymes were used in accordance with the manufacturer's instructions. The primers used are listed in Table SM1. *Escherichia coli* strain TOP10 (Invitrogen) was used as the host strain for all plasmids. The deletion strategy is described in Supporting Information.

Bacterial growth kinetics. Cells were cultured overnight in LB medium at 37°C, and then at 30°C overnight in iron-deficient succinate medium. They were then diluted to 0.1 $OD_{600\ nm}$ units. The suspension (200 μl) was dispensed into individual wells of a 96-well plate (Greiner, PS flat-bottomed microplate). Plates were incubated at 30°C, with shaking, in a TECAN microplate reader (Infinite M200, TECAN) for measurements of OD_{600} at 30 minute-intervals, for 30 h. Each growth curve represents the mean derived from five replicates.

Expression of FpvG and FpvH in* E. coli *and membrane preparations. To construct an overexpressing vector for C-terminal His-tagged *fpvG* expression, a synthetic gene was synthesized by the company GenScript and cloned into the pUC57 vector. The *fpvGHis*$_6$ fragment was than cloned into the pET29a(+) plasmid using the *NdeI* and *XhoI* restriction sites, giving the pET29a(+)-*fpvGHis*$_6$ vector.

To overexpress FpvH with a His tag in the N or C terminus, DNA was amplified by PCR using two sets of primer pairs, His_6FpvH1/2 and FpvH$His_6$1/2 (Supplementary Table 1),

to obtain the His_6*fpvH* and *fpvH*His_6 genes, respectively. These DNA fragments were digested by *BamHI* and *HindIII* and inserted into the pMMB190 vector, linearized with the same enzymes, to get both recombinant plasmids pMMB190His_6*fpvH* and pMMB190*fpvH*His_6.

FpvG C-terminal His-tagged protein was overexpressed in *E. coli* BL21(DE3) cells carrying the pET29a(+)FpvGHis_6 plasmid. Strains *E. coli* BL21(DE3)(pET29a(+)FpvGHis_6) and the control strain BL21(DE3)(pET29a) were used to prepare bacterial membranes containing or not FpvG. After growth in LB, bacteria were re-suspended in 50 mM Tris-HCl pH 8.0 in the presence of 1 mM EDTA and cells were disrupted by sonication. Afterwards, unbroken cells were pelleted during 20 min at 6,700 g. The supernatant was collected and membranes pelleted by centrifugation during 40 min at 125,000 *g* at 4°C. The membranes were re-suspended in 50 mM Tris-HCl pH 8.0 and the protein concentrations were determined using the BCA (Pierce) assay.

We also attempted to express FpvH in *E. coli* BL21(DE3) using the pMMB190FpvHHis_6 or pMMB190His_6FpvH plasmids, but without success.

Purification of FpvC, FpvC$_{mut}$, and FpvF. FpvC and His-tagged FpvF were purified from *E. coli* BL21(DE3) and *P. aeruginosa* strains respectively carrying pET23a-789 or pVEGA6 plasmids as described previously[20] using the protocol detailed in the same reference.

$FpvC_{mut}$ is a mutant of FpvC, with His40, His65, His110, His176, His198, and His249 mutated into Gly and a His-tag at the C-terminal end. To construct an overexpressing vector for $FpvC_{mut}$ production, a synthetic gene was synthesized by the company GenScript and cloned into the pUC57 vector. The *fpvC$_{mut}$* fragment was than cloned into the pET29a(+) plasmid using the *NdeI* and *XhoI* restriction sites, giving the pET29a(+)-*fpvC$_{mut}$* vector. $FpvC_{mut}$ was purified from *E. coli* BL21(DE3)(pET29a(+)-*fpvC$_{mut}$)* strains. *E. coli* cells expressing $FpvC_{mut}$ protein were grown in Luria Bertani (LB)-kanamycin (100 μg.ml) at 37°C

and 220 rpm until the optical density ($OD_{600\ nm}$) of the cultured cells reached 0.6. Expression of the recombinant protein was induced with 2 mM isopropyl-β-D-thiogalactopyranoside (IPTG) at 37°C during 3h. The cells were harvested and washed with 50 mM Tris-HCl pH 8.0, 1 mM EDTA. The pellet was disurpted by sonication, and centrifuged 20 min at 6,700 g to remove unbroken cells. The supernatant was then loaded onto an HisTrap column, the $FpvC_{mut}$ protein was eluted with a linear imidazole gradient. The fractions containing $FpvC_{mut}$ were analyzed on a SDS-PAGE gel and then purified onto a Superdex 200 10/300 GL column, equilibrated with 50 mM Tris-HCl, NaCl 300 mM pH 8.0, to remove aggregates. After purification, all the protein fractions were pooled and concentrated by ultrafiltration at 10,000 g using a 10,000 kDa molecular weight cut off (Amicon, Millipore).

Iron uptake assays and cell fractionation. The PVDI-^{55}Fe complex was prepared at ^{55}Fe concentrations of 20 μM, with a siderophore:iron (mol:mol) ratio of 20:1. Bacteria were grown in CAA medium as described above, then washed with 50 mM Tris-HCl pH 8.0, and diluted to an $OD_{600\ nm}$ of 1. Transport assays were initiated by adding 200 nM PVDI-^{55}Fe to the bacteria. The incorporation of radioactivity into the bacteria was monitored immediately after addition of PVDI-^{55}Fe and after 15 and 30 min incubation, by centrifugation, as previously described.[27] The experiments were repeated with cells pretreated with 200 μM CCCP. This compound inhibits the proton-motive force across the bacterial cell membranes, inhibiting TonB-dependent iron uptake.[21]

For the cell fractionation assay, 25 mL bacterial grown in CAA medium were incubated in the presence of 200 nM PVDI-^{55}Fe at 30°C. After 30 min incubation, periplasmic, cytoplasmic and membrane fractions were isolated as previously described.[28]

Fluorescence spectroscopy (PVDI-Fe dissociation and PVDI recycling experiments). All

measurements were performed using a TECAN microplate reader (Infinite M200, TECAN) for all *in vivo* and *in vitro* assays. Samples were stirred at 30°C in 96-well plates, the excitation wavelength set to 400 nm, and the fluorescence emission measured at 447 nm every 300 ms for the duration of the experiment.

For the *in vitro* PVDI-Fe dissociation experiments, PVDI-Fe was used at a concentration of 20 µM in 200 µL 100 mM acetate ammonium buffer, pH 6.5. PVDI-Fe dissociation was followed at 447 nm in the presence or absence of either 100 mM DTT, 100 mM ascorbic acid, 2 mM, 200 µM or 20 µM ferrozine, 10 µM FpvC, 10 µM FpvF, and 10 µg membranes.

For the *in vivo* PVDI-Fe dissociation experiments, cells grown in CAA or succinate media, as described above, were washed with two volumes of 50 mM Tris-HCl, pH 8.0 and resuspended in the same buffer to a final $OD_{600\ nm}$ of 0.4. PVDI-Fe was added to a concentration of 120 nM and the fluorescence at 447 nm measured. As a control, the same experiments were repeated in the absence of (i) the siderophore or (ii) bacteria.

For the PVDI recycling experiments, bacteria were prepared at $OD_{600\ nm}$ of 1 in a volume of 3 mL. PVDI-Fe was added to the cells to a concentration of 120 nM. 200 µL of the suspension was removed at regular time intervals, the bacteria pelleted, and the fluorescence at 447 nm (excitation wavelength: 400 nm) monitored in 150 µL supernatant. As a control, the same experiments were repeated in the absence of (i) the siderophore or (ii) the bacteria.

ACKNOWLEDGMENTS

This work was partly funded by the *Centre National de la Recherche Scientifique* and a grant from the ANR (*Agence Nationale de Recherche*, *IronPath* ANR-12-BSV8-0007-01). B. Roche was paid by Roche Phamaceutical.

Supporting Information Available: This material is available free of charge *via* the Internet.

REFERENCES

1. Cunrath, O., Geoffroy, V. A., and Schalk, I. J. (2015) Metallome of *Pseudomonas aeruginosa*: a role for siderophores. *Env. Microbiol*. *18*, 3258–3267

2. Boukhalfa, H., and Crumbliss, A. L. (2002) Chemical aspects od siderophore mediated iron transport. *Biometals 15*, 325–39.

3. Albrecht-Gary, A. M., Blanc, S., Rochel, N., Ocacktan, A. Z., and Abdallah, M. A. (1994) Bacterial iron transport: coordination properties of pyoverdin PaA, a peptidic siderophore of *Pseudomonas aeruginosa*. *Inorg Chem 33*, 6391–6402.

4. Raymond, K. N., Dertz, E. A., and Kim, S. S. (2003) Enterobactin: an archetype for microbial iron transport. *Proc Natl Acad Sci U A 100*, 3584–8.

5. Ye, L., Ballet, S., Hildebrand, F., Laus, G., Guillemyn, K., Raes, J., Matthijs, S., Martins, J., and Cornelis, P. (2013) A combinatorial approach to the structure elucidation of a pyoverdine siderophore produced by a *Pseudomonas putida* isolate and the use of pyoverdine as a taxonomic marker for typing *P. putida* subspecies. *Biometals Int. J. Role Met. Ions Biol. Biochem. Med. 26*, 561–575.

6. Demange, P., Wendenbaum, S., Linget, C., Mertz, C., Cung, M. T., and Dell, A., Abdallah, M. A. (1990) Bacterial siderophores: structure and NMR assigment of pyoverdins PaA, siderophores of *Pseudomonas aeruginosa* ATCC 15692. *Biol Met. 3*, 155–170.

7. Schalk, I. J., Mislin, G. L. A., and Brillet, K. (2012) Structure, function and binding selectivity and stereoselectivity of siderophore-iron outer membrane transporters. *Curr. Top. Membr. 69*, 37–66.

8. Poole, K., Neshat, S., and Heinrichs, D. (1991) Pyoverdine-mediated iron transport in *Pseudomonas aeruginosa*: involvement of a high-molecular-mass outer membrane protein. *FEMS Microbiol Lett 62*, 1–5.

9. Wirth, C., Meyer-Klaucke, W., Pattus, F., and Cobessi, D. (2007) From the periplasmic signaling domain to the extracellular face of an outer membrane signal transducer of *Pseudomonas aeruginosa*: crystal structure of the ferric pyoverdine outer membrane receptor. *J Mol Biol 68*, 398–406.

10. Ghysels, B., Dieu, B. T., Beatson, S. A., Pirnay, J. P., Ochsner, U. A., Vasil, M. L., and Cornelis, P. (2004) FpvB, an alternative type I ferripyoverdine receptor of *Pseudomonas aeruginosa*. *Microbiology 150*, 1671–80.

11. Postle, K., and Larsen, R. A. (2007) TonB-dependent energy transduction between outer and cytoplasmic membranes. *Biometals 20*, 453–65.

12. Schalk, I. J., and Guillon, L. (2013) Fate of ferrisiderophores after import across bacterial outer membranes: different iron release strategies are observed in the cytoplasm or periplasm depending on the siderophore pathways. *Amino Acids 44*, 1267–77.

13. Greenwald, J., Hoegy, F., Nader, M., Journet, L., Mislin, G. L. A., Graumann, P. L., and Schalk, I. J. (2007) Real-time FRET visualization of ferric-pyoverdine uptake in *Pseudomonas aeruginosa*: a role for ferrous iron. *J Biol Chem 282*, 2987–2995.

14. Yeterian, E., Martin, L. W., Lamont, I. L., and Schalk, I. J. (2010) An efflux pump is required for siderophore recycling by *Pseudomonas aeruginosa*. *Env. Microbiol Rep. 2*, 412–418.

15. Marshall, B., Stintzi, A., Gilmour, C., Meyer, J.-M., and Poole, K. (2009) Citrate-mediated iron uptake in *Pseudomonas aeruginosa*: involvement of the citrate-inducible FecA receptor and the FeoB ferrous iron transporter. *Microbiol. Read. Engl. 155*, 305–315.

16. Hartman, A., and Braun, V. (1980) Iron transport in Escherichia coli: uptake and modification of ferrichrome. *J Bacteriol 143*, 246–55.

17. Matzanke, B. F., Anemuller, S., Schunemann, V., Trautwein, A. X., and Hantke, K. (2004) FhuF, part of a siderophore-reductase system. *Biochemistry (Mosc.) 43*, 1386–92.

18. Schalk, I. J., Abdallah, M. A., and Pattus, F. (2002) Recycling of pyoverdin on the FpvA receptor after ferric pyoverdin uptake and dissociation in *Pseudomonas aeruginosa*. *Biochemistry (Mosc.) 41*, 1663–1671.

19. Imperi, F., Tiburzi, F., and Visca, P. (2009) Molecular basis of pyoverdine siderophore recycling in *Pseudomonas aeruginosa*. *Proc Natl Acad Sci U A 106*, 20440–5.

20. Brillet, K., Ruffenach, F., Adams, H., Journet, L., Gasser, V., Hoegy, F., Guillon, L., Hannauer, M., Page, A., and Schalk, I. J. (2012) An ABC transporter with two periplasmic binding proteins involved in iron acquisition in *Pseudomonas aeruginosa*. *ACS Chem Biol 7*, 2036–45.

21. Clément, E., Mesini, P. J., Pattus, F., Abdallah, M. A., and Schalk, I. J. (2004) The binding mechanism of pyoverdin with the outer membrane receptor FpvA in *Pseudomonas aeruginosa* is dependent on its iron-loaded status. *Biochemistry (Mosc.) 43*, 7954–65.

22. Schalk, I. J., Kyslik, P., Prome, D., van Dorsselaer, A., Poole, K., Abdallah, M. A., and Pattus, F. (1999) Copurification of the FpvA ferric pyoverdin receptor of *Pseudomonas aeruginosa* with its iron-free ligand: implications for siderophore-mediated iron transport. *Biochemistry (Mosc.) 38*, 9357–65.

23. Folschweiller, N., Gallay, J., Vincent, M., Abdallah, M. A., Pattus, F., and Schalk, I. J. (2002) The interaction between pyoverdin and its outer membrane receptor in *Pseudomonas aeruginosa* leads to different conformers: a time-resolved fluorescence study. *Biochemistry (Mosc.) 41*, 14591–601.

24. Stookey, L. L. (1970) Ferrozine-A New Spectrophotometric Reagent for Iron. *Anal. Chem. 42*, 779–781.

25. Xiao, R., and Kisaalita, W. S. (1998) Fluorescent pseudomonad pyoverdines bind and oxidize ferrous ion. *Appl Env. Microbiol 64*, 1472–6.

26. Albrechtgary, A. M., Blanc, S., Rochel, N., Ocaktan, A. Z., and Abdallah, M. A. (1994)

Bacterial iron transport - coordination properties of pyoverdin Paa, a peptidic siderophore of *Pseudomonas-aeruginosa*. *Inorg. Chem. 33*, 6391–6402.

27. Hoegy, F., and Schalk, I. J. (2014) Monitoring iron uptake by siderophores. *Methods Mol Biol 1149*, 337–46.

28. Cunrath, O., Gasser, V., Hoegy, F., Reimmann, C., Guillon, L., and Schalk, I. J. (2015) A cell biological view of the siderophore pyochelin iron uptake pathway in *Pseudomonas aeruginosa*. *Env. Microbiol 17*, 171–85.

29. Stover, C. K., Pham, X. Q., Erwin, A. L., Mizoguchi, S. D., Warrener, P., Hickey, M. J., Brinkman, F. S., Hufnagle, W. O., Kowalik, D. J., Lagrou, M., Garber, R. L., Goltry, L., Tolentino, E., Westbrock-Wadman, S., Yuan, Y., Brody, L. L., Coulter, S. N., Folger, K. R., Kas, A., Larbig, K., Lim, R., Smith, K., Spencer, D., Wong, G. K., Wu, Z., Paulsen, I. T., Reizer, J., Saier, M. H., Hancock, R. E., Lory, S., and Olson, M. V. (2000) Complete genome sequence of Pseudomonas aeruginosa PAO1, an opportunistic pathogen. *Nature 406*, 959–64.

30. Shirley, M., and Lamont, I. L. (2009) Role of TonB1 in pyoverdine-mediated signaling in *Pseudomonas aeruginosa*. *J Bacteriol 191*, 5634–40.

31. Voisard, C., Bull, C., Keel, C., Laville, J., Maurhofer, M., Schnider, U., Défago, G., and Haas, D. (1994) Biocontrol of root diseases by *Pseudomonas fluorescens* CHAO: current concepts and experimental approaches, in *Molecular Ecology of Rhizosphere Microorganisms* (O'Gara, F., Dowling, D. N., and Boesten, Eds.), pp 67–89. VCH, Weinheim, Germany.

32. Morales, V. M., Backman, A., and Bagdasarian, M. (1991) A series of wide-host-range low-copy-number vectors that allow direct screening for recombinants. *Gene 97*, 39–47.

Strains and plasmids	Collection ID	Relevant characteristics	Source or references
Pseudomonas aeruginosa			
PAO1	PAO1	Wild-type strain	[29]
Δ*pvdF*	PAS047	PAO1; *pvdF* chromosomally deleted	[1]
Δ*pvdF*Δ*fpvA*	PAS150	PAO1; *pvdF* and *fpvA* chromosomally deleted	[30]
Δ*pvdF*Δ*fpvG*	PAS279	PAO1; *pvdF* and *fpvG* chromosomally deleted	This study
Δ*pvdF*Δ*fpvG*(pMMB*fpvG*)	PAS341	Derivative of Δ*pvdF*Δ*fpvG* transformed with pMMB*fpvG*	This study
Δ*pvdF*Δ*fpvH*	PAS280	PAO1; *pvdF* and *fpvH* chromosomally deleted	This study
Δ*pvdF*Δ*fpvH*(pMMB*fpvH)*	PAS342	Derivative of Δ*pvd*Δ*fpvH* transformed with pMMB*fpvH*	This study
Δ*pvdF*Δ*fpvJ*	PAS281	PAO1; *pvdF* and *fpvJ* chromosomally deleted	This study
Δ*pvdF*Δ*fpvK*	PAS336	PAO1; *pvdF* and *fpvK* chromosomally deleted	This study
Δ*pvdF*Δ*fpvGHJK*	PAS337	PAO1; *pvdF, fpvG, fpvH, fpvJ* and *fpvK* chromosomally deleted	This study
Δ*pvdF*Δ*fpvC*	PAS315	PAO1; *pvdF* and *fpvC* chromosomally deleted	This study
Δ*pvdF*Δ*fpvDE*	PAS317	PAO1; *pvdF, fpvD* and *fpvE* chromosomally deleted	This study
Δ*pvdF*Δ*fpvF*	PAS314	PAO1; *pvdF* and *FpvF* chromosomally deleted	This study
Δ*pvdF*Δ*fpvCDEF*	PAS318	PAO1; *pvdF*, *fpvC, fpvD, fpvE* and *fpvF* chromosomally deleted	This study
Δ*pvdF*ΔfpvCDEF(pMMB*fpvCDEF*)	PAS323	Derivative of PAO1 Δ*pvdF*Δ*fpvCDEF transformed with* pMMB*fpvCDEF*	This study
Escherichia coli			
TOP10		F- mcrA Δ(mrr-hsdRMS-mcrBC) φ80lacZΔM15 ΔlacX74 nupG recA1 araD139 Δ(ara-leu)7697 galE15 galK16 rpsL(Str^R) endA1 λ^-	Invitrogen
BL21(DE3)		*F– ompT hsdS_B(r_B–m_B–) gal dcm (λ* DE3)	Novagen
Plasmids			
pME3088		Suicide vector; TcR; ColE1 replicon; *EcoRI KpnI DraII XhoI HindIII* polylinker	[31]
pMMB190		Complementation vector; AmpR	[32]
pMEΔ*fpvG*	pGG7	pME3088 *carrying the sequence to delete fpvG*	This study
pMEΔ*fpvH*	pFH2	pME3088 *carrying the sequence to delete fpvH*	This study
pMEΔ*fpvJ*	pFH3	pME3088 *carrying the sequence to delete fpvJ*	This study

pMEΔ*fpvK*	pFH4	pME3088 *carrying the sequence to delete fpvK*	This study
pMEΔ*fpvGHJK*	pGG8	pME3088 *carrying the sequence to delete fpvGHJK*	This study
pMEΔ*fpvC*	pGG2	pME3088 *carrying the sequence to delete fpvC*	This study
pMEΔ*fpvDE*	pGG3	pME3088 *carrying the sequence to delete fpvDE*	This study
pMEΔ*fpvF*	pGG1	pME3088 *carrying the sequence to delete fpvF*	This study
pMEΔ*fpvCDEF*	pLJ76	pME3088 *carrying the sequence to delete fpvCDEF*	[20]
pMMB*fpvG*	pGG10	pMMB190 carrying *fpvG*	This study
pMMB*fpvH*	pGG11	pMMB190 carrying *fpvH*	This study
pET29a	pET29a	vector carry an N-terminal S•Tag™/thrombin configuration plus a C-terminal His•Tag® sequence	Novagen
pET29a(+)*fpvG*His_6	pET29a(+)*fpvG*His_6	pET29 carrying a C-terminal His-tagged *fpvG*	This study
pMMB190*fpvH*His_6	pGG12	pMMB190 carrying a C-terminal His-tagged *fpvH*	This study
pMMB190His_6*fpvH*	pGG13	pMMB190 carrying a N-terminal His-tagged *fpvH*	This study
pET23a-789	pET23a-789	pET23 carrying *fpvC*	[20]
pVEGA6	pVEGA6	pMMB190 carrying EcoRI-HindIII fragment containing *fpvF*-6His	[20]
pET29a(+)-$fpvC_{mut}$	pET29a(+)-$fpvC_{mut}$	pET29 carrying a C-terminal His-tagged *fpvC* with the His 40, 65, 110, 176, 198, 249 mutated into Gly	This study

Table 1: Strains and plasmids used in this study.

FIGURES WITH LEGENDS

Figure 1: a) Organization of the PA2403-10 genes in the *P. aeruginosa* PAO1 genome. IMP, Inner Membrane Protein; PP, periplasmic protein; and PBP, periplasmic binding protein. See in Supporting information for the predicted membrane topology (Supplementary Figure 1).

b) Putative secondary structure of FpvG (PA2403). The black arrows show the β-sheets and the gray bars the α-helices (light gray for the transmembrane regions).

c) Sequence of the periplasmic binding protein FpvC with a C-terminal His tag. The His residues potentially involved in metal chelation[20] and mutated into Gly in $FpvC_{mut}$ are shown in red.

Figure 2: a) ^{55}Fe uptake in *P. aeruginosa* strains after incubation with PVDI-^{55}Fe. Δ*pvdF*, a PVDI-negative strain, and its corresponding deletion mutants Δ*pvdF*Δ*fpvGHJK*, Δ*pvdF*Δ*fpvG*, Δ*pvdF*Δ*fpvH*, Δ*pvdF*Δ*fpvJ,* Δ*pvdF*Δ*fpvK,* as well as Δ*pvdF*Δ*fpvA*, its *fpvA* deletion mutant (grown in CAA medium), were incubated with 200 nM PVDI-^{55}Fe for 15 or 30 min. The cells were then pelleted and the radioactivity accumulated in the bacteria counted. The results are expressed as pmol of PVD-^{55}Fe transported per mL of cells at an $OD_{600\ nm}$ of 1. The error bars represent the standard deviations of the mean of three independent experiments.

b) ^{55}Fe repartition in the cell compartments of *P. aeruginosa* strains after incubation with PVDI-^{55}Fe. Δ*pvdF* and its corresponding deletion mutants Δ*pvdF*Δ*fpvA*, Δ*pvdF*Δ*fpvGHJK*, and Δ*pvdF*Δ*fpvG*, were first grown in CAA medium and then incubated with 200 nM PVDI-^{55}Fe for 30 min. The cells were then pelleted, the periplasm, cytoplasm and membrane fractions isolated for each strain as described in Materials and Methods, and

the amount of ^{55}Fe present measured. The results are expressed as the percentage of pmol of ^{55}Fe incubated with the strains. The errors bars represent the standard deviation of the mean of three independent experiments.

Figure 3: a and b) *In vivo* PVDI-Fe dissociation kinetics, measured by direct excitation of PVDI. Cells (Δ*pvdF*, Δ*pvdF*Δ*fpvG*, Δ*pvdF*Δ*fpvH*, Δ*pvdF*Δ*fpvJ*, Δ*pvdF*Δ*fpvK*, Δ*pvdF*Δ*fpvGHJK*, and Δ*pvdF*Δ*fpvA* cells for panel A and Δ*pvdF*, Δ*pvdF*Δ*fpvC*, Δ*pvdF*Δ*fpvDE*, Δ*pvdF*Δ*fpvF*, Δ*pvdF*Δ*fpvCDEF*, and Δ*pvdF*Δ*fpvA* for panel B) were washed and resuspended to an $OD_{600\ nm}$ of 0.4 in 50 mM Tris-HCl, pH 8.0, and incubated at 30°C. The change in PVDI fluorescence (excitation set at 400 nm) was monitored by measuring the emission of fluorescence at 447 nm, every 300 ms, for 60 min, in a TECAN microplate reader. After 10 min, 120 nM PVDI-Fe was added as indicated by the black vertical line. The kinetics experiments were repeated in the absence of PVDI-Fe for all strains tested and no increase of fluorescence was observed (data not shown).

c and d) PVDI recycling after iron uptake measured by fluorescence. Bacterial cells (Δ*pvdF*, Δ*pvdF*Δ*fpvG*, Δ*pvdF*Δ*fpvH*, Δ*pvdF*Δ*fpvJ*, Δ*pvdF*Δ*fpvK*, Δ*pvdF*Δ*fpvGHJK*, and Δ*pvdF*Δ*fpvA* cells for panel C and Δ*pvdF*, Δ*pvdF*Δ*fpvC*, Δ*pvdF*Δ*fpvDE*, Δ*pvdF*Δ*fpvF*, Δ*pvdF*Δ*fpvCDEF*, and Δ*pvdF*Δ*fpvA* for panel D) were incubated to an $OD_{600\ nm}$ of 1 in 50 mM Tris-HCl (pH 8.0) buffer in the presence of 120 nM PVDI-Fe at 30°C. Aliquots (200 µL) were collected at intervals, the cells removed by centrifugation, and the fluorescence in 150 µL supernatant measured at 447 nm (λ_{ext} = 400 nm) using a TECAN microplate reader. The experiment was repeated for all strains in the absence of PVDI-Fe addition (data not shown) and no time-dependent increase of fluorescence was observed.

All the kinetics experiments presented in panels A-D were performed three times and equivalent kinetics were observed.

Figure 4: Dissociation of PVDI-Fe *in vitro*. For all shown experiments, 20 μM PVDI-Fe was incubated in 100 mM ammonium acetate buffer (pH 6.5**)** in the absence or presence of 100 mM DTT, 100 mM ascorbic acid, 200 μM ferrozine, 10 μM FpvC, 10 μM FpvF, 10 μg membranes of BL21(DE3) or BL21(DE3)(pET29a(+)FpvGHis_6) cells overexpressing FpvG. For panel D, ferrozine was added to 20 μM (1 equivalent compared to the PVDI-Fe concentration), 200 μM (10 eq.), or 2 mM (100 eq.). For all experiments, the change in fluorescence (excitation set at 400 nm) was monitored by measuring the emission of fluorescence at 447 nm, every second, for 60 min. For panel A, the kinetics shown by the solid lines were measured by emission of fluorescence at 447 nm and those shown by the dotted lines by absorbance at 562 nm. F_0 = fluorescence at time t_0 and F = fluorescence at time t, A_0 = absorbance at time t_0 and A = absorbance at time t. The various compounds added for each experiment are specified on the different panels with the corresponding colors, except for several curves corresponding to controls in panel A: gray curve, 100 mM ammonium acetate buffer (pH 6.5) alone; dark gray curve, PVDI-Fe alone; black curve, DTT alone; brown curve, ferrozine alone; khaki curve, DTT incubated with ferrozine alone (no PVDI-Fe).

Figure 5: Western blot analyses of membranes of BL21(DE3) *E. coli* cells expressing FpvG. The membranes were prepared as described in Materials and Methods and 15 μg of proteins were loaded for each lane. Lane 2, soluble (cytoplasm and periplasm) fraction; lane 3: membrane fraction. His tagged FpvG (MW of 45.9 kDa) was detected using a rabbit anti-His monoclonal antibody (GeneTex).

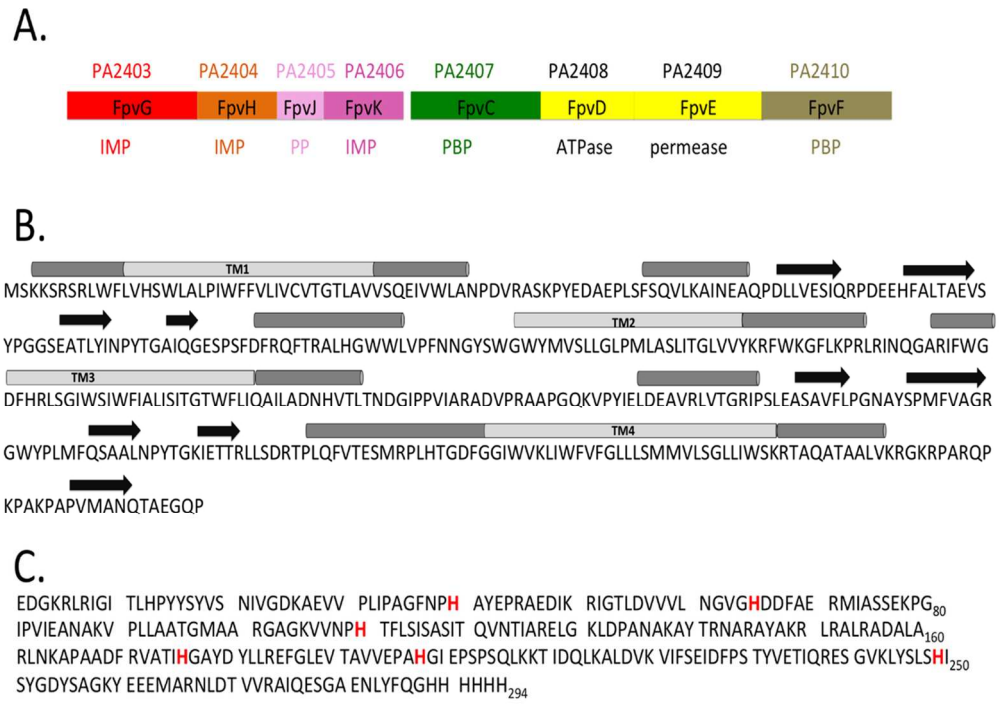

Figure 1: a) Organization of the PA2403-10 genes in the P. aeruginosa PAO1 genome. IMP, Inner Membrane Protein; PP, periplasmic protein; and PBP, periplasmic binding protein. See in Supporting information for the predicted membrane topology (Supplementary Figure 1).
b) Putative secondary structure of FpvG (PA2403). The black arrows show the β-sheets and the gray bars the α-helices (light gray for the transmembrane regions).
c) Sequence of the periplasmic binding protein FpvC with a C-terminal His tag. The His residues potentially involved in metal chelation20 and mutated into Gly in FpvCmut are shown in red.
Figure 1
104x78mm (300 x 300 DPI)

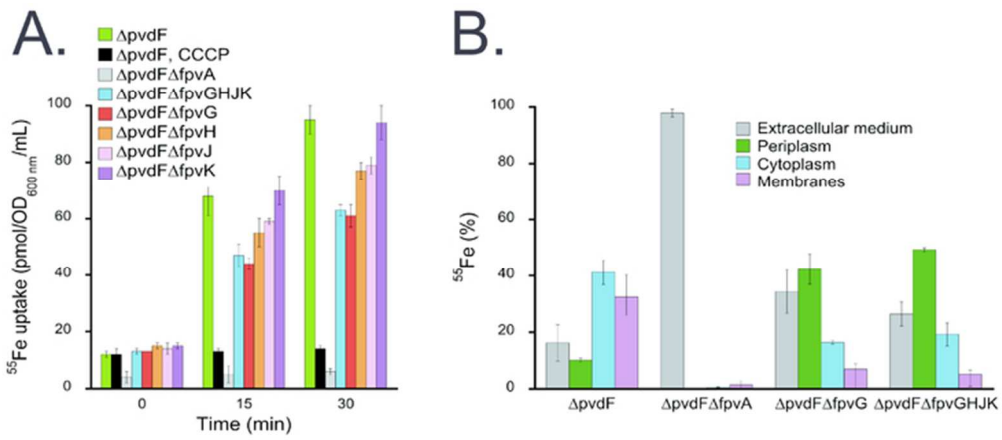

Figure 2: a) 55Fe uptake in P. aeruginosa strains after incubation with PVDI-55Fe. ΔpvdF, a PVDI-negative strain, and its corresponding deletion mutants ΔpvdFΔfpvGHJK, ΔpvdFΔfpvG, ΔpvdFΔfpvH, ΔpvdFΔfpvJ, ΔpvdFΔfpvK, as well as ΔpvdFΔfpvA, its fpvA deletion mutant (grown in CAA medium), were incubated with 200 nM PVDI-55Fe for 15 or 30 min. The cells were then pelleted and the radioactivity accumulated in the bacteria counted. The results are expressed as pmol of PVD-55Fe transported per mL of cells at an OD600 nm of 1. The error bars represent the standard deviations of the mean of three independent experiments. b) 55Fe repartition in the cell compartments of P. aeruginosa strains after incubation with PVDI-55Fe. ΔpvdF and its corresponding deletion mutants ΔpvdFΔfpvA, ΔpvdFΔfpvGHJK, and ΔpvdFΔfpvG, were first grown in CAA medium and then incubated with 200 nM PVDI-55Fe for 30 min. The cells were then pelleted, the periplasm, cytoplasm and membrane fractions isolated for each strain as described in Materials and Methods, and the amount of 55Fe present measured. The results are expressed as the percentage of pmol of 55Fe incubated with the strains. The errors bars represent the standard deviation of the mean of three independent experiments.
Figure 2
61x27mm (300 x 300 DPI)

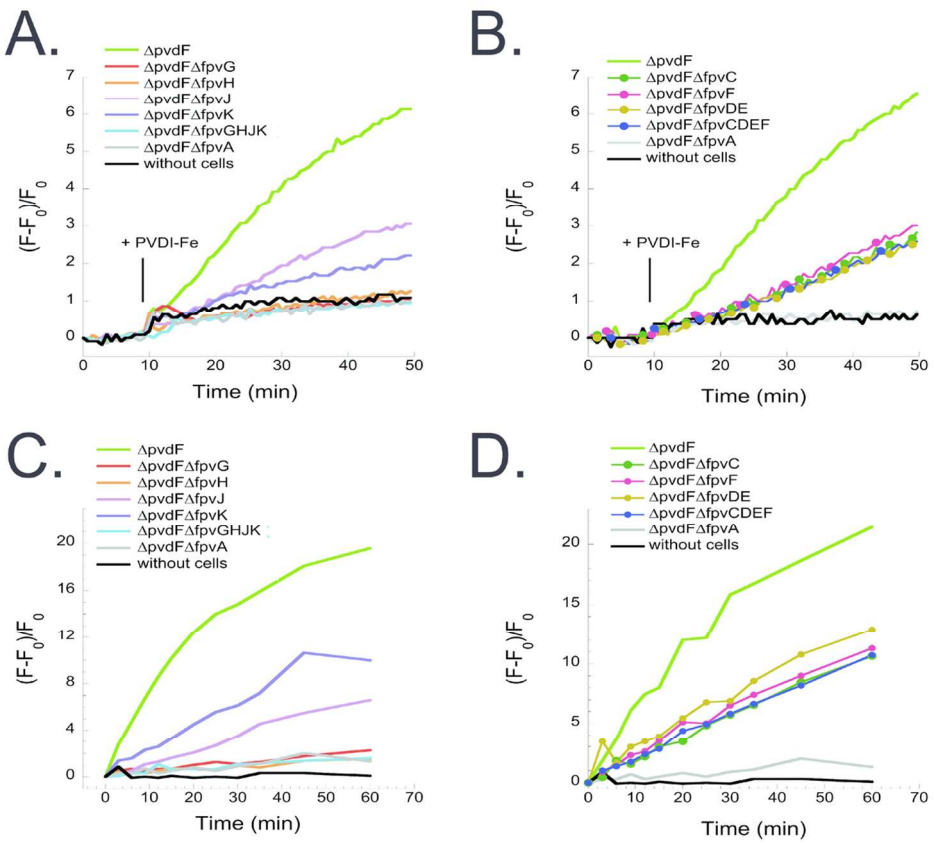

Figure 3: a and b) In vivo PVDI-Fe dissociation kinetics, measured by direct excitation of PVDI. Cells (ΔpvdF, ΔpvdFΔfpvG, ΔpvdFΔfpvH, ΔpvdFΔfpvJ, ΔpvdFΔfpvK, ΔpvdFΔfpvGHJK, and ΔpvdFΔfpvA cells for panel A and ΔpvdF, ΔpvdFΔfpvC, ΔpvdFΔfpvDE, ΔpvdFΔfpvF, ΔpvdFΔfpvCDEF, and ΔpvdFΔfpvA for panel B) were washed and resuspended to an OD600 nm of 0.4 in 50 mM Tris-HCl, pH 8.0, and incubated at 30°C. The change in PVDI fluorescence (excitation set at 400 nm) was monitored by measuring the emission of fluorescence at 447 nm, every 300 ms, for 60 min, in a TECAN microplate reader. After 10 min, 120 nM PVDI-Fe was added as indicated by the black vertical line. The kinetics experiments were repeated in the absence of PVDI-Fe for all strains tested and no increase of fluorescence was observed (data not shown). c and d) PVDI recycling after iron uptake measured by fluorescence. Bacterial cells (ΔpvdF, ΔpvdFΔfpvG, ΔpvdFΔfpvH, ΔpvdFΔfpvJ, ΔpvdFΔfpvK, ΔpvdFΔfpvGHJK, and ΔpvdFΔfpvA cells for panel C and ΔpvdF, ΔpvdFΔfpvC, ΔpvdFΔfpvDE, ΔpvdFΔfpvF, ΔpvdFΔfpvCDEF, and ΔpvdFΔfpvA for panel D) were incubated to an OD600 nm of 1 in 50 mM Tris-HCl (pH 8.0) buffer in the presence of 120 nM PVDI-Fe at 30°C. Aliquots (200 µL) were collected at intervals, the cells removed by centrifugation, and the fluorescence in 150 µL supernatant measured at 447 nm (λext = 400 nm) using a TECAN microplate reader. The experiment was repeated for all strains in the absence of PVDI-Fe addition (data not shown) and no time-dependent increase of fluorescence was observed.
All the kinetics experiments presented in panels A-D were performed three times and equivalent kinetics were observed.
Figure 3
119x101mm (300 x 300 DPI)

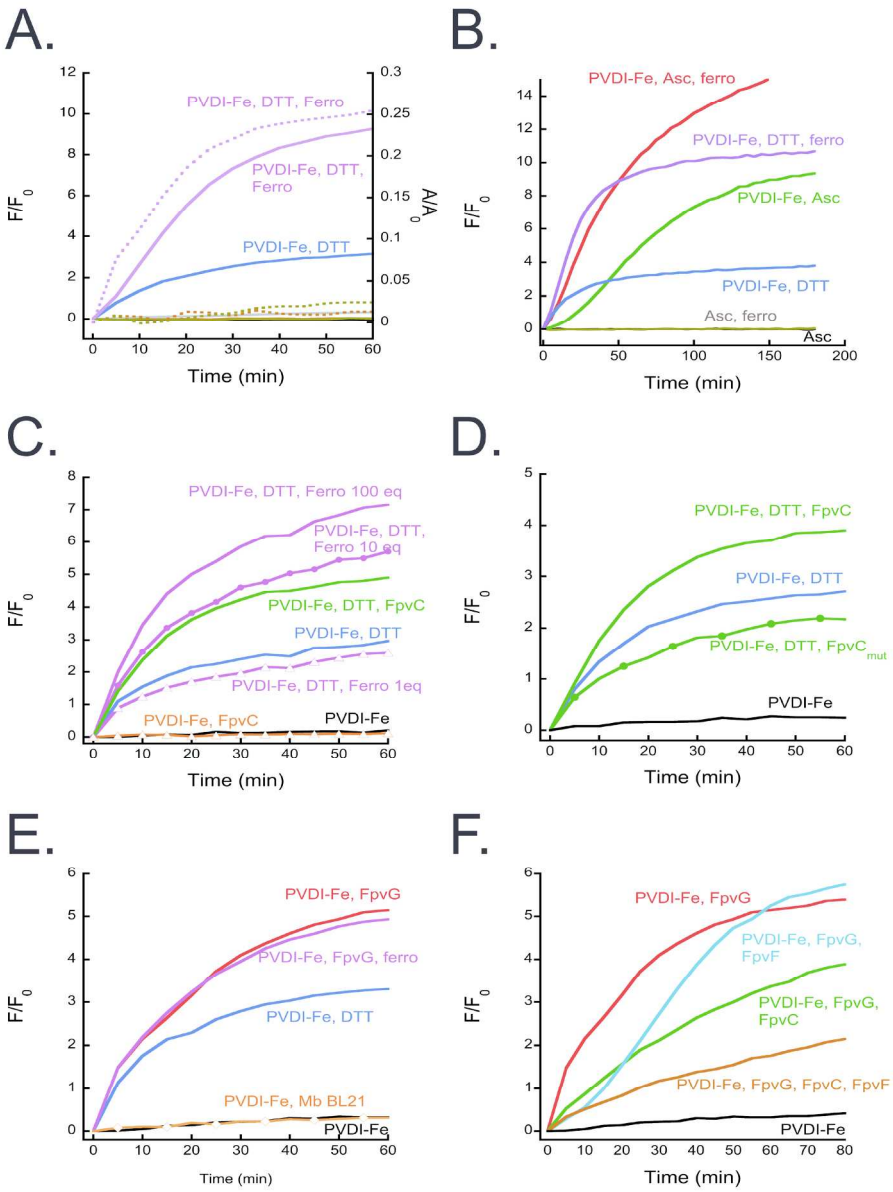

Figure 4: Dissociation of PVDI-Fe in vitro. For all shown experiments, 20 µM PVDI-Fe was incubated in 100 mM ammonium acetate buffer (pH 6.5) in the absence or presence of 100 mM DTT, 100 mM ascorbic acid, 200 µM ferrozine, 10 µM FpvC, 10 µM FpvF, 10 µg membranes of BL21(DE3) or BL21(DE3)(pET29a(+)FpvGHis6) cells overexpressing FpvG. For panel D, ferrozine was added to 20 µM (1 equivalent compared to the PVDI-Fe concentration), 200 µM (10 eq.), or 2 mM (100 eq.). For all experiments, the change in fluorescence (excitation set at 400 nm) was monitored by measuring the emission of fluorescence at 447 nm, every second, for 60 min. For panel A, the kinetics shown by the solid lines were measured by emission of fluorescence at 447 nm and those shown by the dotted lines by absorbance at 562 nm. F0 = fluorescence at time t0 and F = fluorescence at time t, A0 = absorbance at time t0 and A = absorbance at time t. The various compounds added for each experiment are specified on the different panels with the corresponding colors, except for several curves corresponding to controls in panel A: gray curve, 100 mM ammonium acetate buffer (pH 6.5) alone; dark gray curve, PVDI-Fe alone; black curve, DTT alone; brown curve, ferrozine alone; khaki curve, DTT incubated with ferrozine alone (no

PVDI-Fe).
Figure 4
183x241mm (300 x 300 DPI)

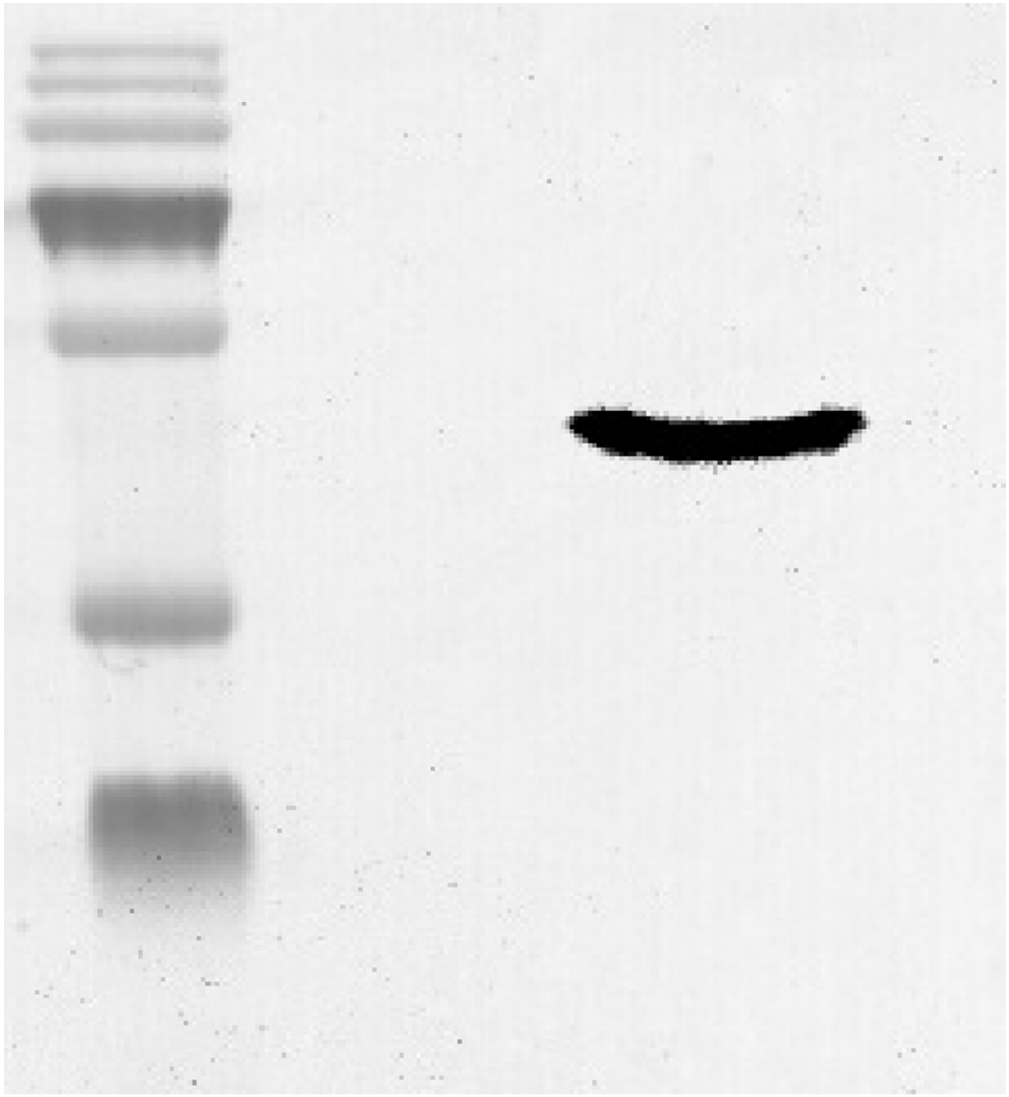

Figure 5: Western blot analyses of membranes of BL21(DE3) E. coli cells expressing FpvG. The membranes were prepared as described in Materials and Methods and 15 µg of proteins were loaded for each lane. Lane 2, soluble (cytoplasm and periplasm) fraction; lane 3: membrane fraction. His tagged FpvG (MW of 45.9 kDa) was detected using a rabbit anti-His monoclonal antibody (GeneTex).
Figure 5
73x79mm (300 x 300 DPI)

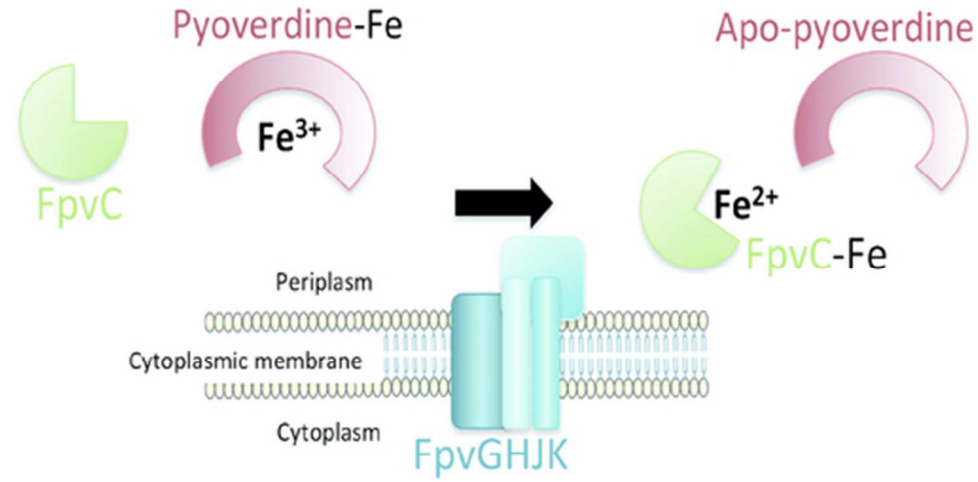

Fe dissociation from siderophore pyoverdine in *P. aeruginosa* periplasm

Graphical abstract
44x25mm (300 x 300 DPI)